Thermally perturbed barodiffusion in a binary liquid mixture

F. B. Hicks, Thomas C. Van Vechten, and Carl Franck
Laboratory of Atomic and Solid State Physics and Materials Science Center, Cornell University, Ithaca, New York 14853-2501
(Received 12 June 1996)

In a binary liquid, the existence of a gravity-induced concentration gradient (the barodiffusion gradient) is a requirement for the system to be in equilibrium. In order to study the effect of forces which could drive such a system from equilibrium, we observe the long-time evolution of gravity-induced concentration gradients in the presence of small perturbing horizontal temperature gradients ($\leqslant$ 85 mK/cm) in a system of aniline and cyclohexane near its critical point. These measurements are unique since previous studies of gravity-induced concentration gradients in binary liquids have focused only on fast developing gradients created by sedimentation or on the measurement of equilibrium barodiffusion. Our results reveal large variations in the steady state concentration gradients even in the absence of applied temperature gradients, suggesting that very small temperature gradients may cause significant fluctuations in a binary liquid system. Additionally, as the applied temperature gradient increases, the growth of the concentration gradients slows and fluctuations on time scales much shorter than the expected diffusion time appear. [S1063-651X(97)14402-6]

PACS number(s): 66.10.Cb, 47.27.Te, 61.20.−p, 05.70.Ln

I. INTRODUCTION

A central motivation of this work is a desire to investigate the limits of equilibrium in a binary liquid mixture. This question is important because it has been shown that in a binary liquid, the structure of the bulk can significantly influence localized structures, such as gravity-thinned wetting layers [1], so that measurement of local equilibrium properties requires bulk equilibrium. Apart from one effort to estimate the size of accidental temperature gradients necessary to drive a binary liquid from equilibrium [2], the warning of Kayser, Moldover, and Schmidt to avoid convective effects that can uncontrollably drive a system from equilibrium [3] has not been heeded in recent work on gravity thinned wetting. Some experimental workers have mentioned the possible effects of temperature gradients. For instance, Bonn and co-workers have reported that large temperature gradients resulting from applied temperature ramps can cause rapid fluctuations in the optical signal used as a probe of wetting layer thicknesses [4]. These and other recent studies, however, do not estimate the possible size or influence of unintended stray temperature gradients (probably the main source of these convective effects) in their systems [5,6]. The experiment reported here attempts to investigate the effect of thermally induced convection on one bulk structure which arises in a binary liquid, the barodiffusion gradient.

In a binary liquid, a requirement for being in equilibrium in a gravitational field is the existence of the barodiffusion gradient, which arises when the two pure components of the (incompressible) mixture have different densities. Without gravity, a single phase of a binary liquid will be well mixed and homogeneous; however, if the same mixture is held at rest in a gravitational field, it will be energetically favorable for the molecules of the denser species to be found lower in the mixture, and a concentration gradient will tend to form. This process, resulting from the pressure gradient provided by gravity, leads to a mass flux in the system. Including the effects of concentration and thermal (Soret) diffusion, the total flux of one component **j** in the liquid mixture will be [7]

$$\mathbf{j}=-\rho D\left(\nabla c+\frac{k_T}{T}\nabla T+\frac{k_p}{p}\nabla p\right), \tag{1}$$

where ρ is the mass density, D is the mutual diffusion coefficient, c is the mass fraction concentration of the component, p and T are the pressure and temperature, and k_p and k_T are the barodiffusion and thermodiffusion ratios. Traditionally, the flux due to the pressure term is referred to as sedimentation or pressure diffusion; we choose to refer to the long-time interaction between sedimentation and concentration diffusion as barodiffusion. In equilibrium with no temperature gradients, the gradient resulting from this interaction, the barodiffusion gradient, will be

$$\nabla c=-\frac{k_p}{p}\nabla p=\frac{k_p}{p}\rho\mathbf{g}, \tag{2}$$

the second equality holding since the earth's gravitational field **g** provides the pressure gradient in this experiment.

As a critical composition binary liquid approaches its critical temperature T_c, the diffusion coefficient vanishes as $D\sim|T-T_c|^{\gamma-\nu}$ with $\gamma-\nu\approx 0.6$, and both the barodiffusion ratio and gradient diverge as $k_p\sim|\nabla c|\sim|T-T_c|^{-\gamma}$ with $\gamma\approx 1.2$ [8]. Since the product Dk_p also diverges near the critical point, the rate of sedimentation diverges while the rate of diffusion tends to zero.

Once the barodiffusion gradient has formed in a binary liquid, one can imagine that an effective way to destroy the gradient (and therefore drive the system from equilibrium) is to stir the mixture. Two possible ways of introducing this stirring are by agitating the mixture (mechanical stirring) or by imposing temperature gradients which can create buoyancy-driven convection (''thermal'' stirring). While vertical temperature gradients either stabilize a liquid (heating from the top) or must cross some threshold to introduce convection (the Rayleigh-Bénard instability to heating from the bottom), an incompressible liquid is always unstable to heating from the side [9]. Thus even very small horizontal temperature gradients could be effective in driving a mixture

from equilibrium. Accordingly, we choose to use horizontal temperature gradients to provide the thermal stirring in the present experiment.

Considering a mixture in which both barodiffusion and convective stirring occur, each process will have its own characteristic time scale, τ_D for barodiffusion [10] and τ_c for convection:

$$\tau_D = \frac{L^2}{\pi^2 D}; \quad \tau_c = \frac{L}{U_c}. \tag{3}$$

These time scales depend on a characteristic length L (the height of the sample), the mutual diffusion coefficient D introduced in Eq. (1), and U_c, a characteristic velocity of the flow field introduced by stirring. We are interested in the relative rates of diffusion and convection, which can be described by the Péclet number $\mathrm{Pe} = \tau_D / \tau_c$. When $\mathrm{Pe} < 1$ ($\tau_D < \tau_c$), diffusion will be the faster process, and intuitively one expects the barodiffusion gradient will be able to form. Likewise, when $\mathrm{Pe} > 1$ ($\tau_D > \tau_c$), the stirring will be faster, and one expects the barodiffusion gradient will be destroyed. So one can propose that a great enough amount of stirring will prevent a binary liquid system from reaching equilibrium, but with weaker stirring, the barodiffusion gradient may not be significantly modified, so that the system will reach a state of effective equilibrium [2].

Motivated by these considerations, Van Vechten and Franck modified Hart's solution of the Navier-Stokes equations for a binary liquid mixture confined to a tall slot [11] in order to predict the size of temperature gradients which could drive a binary liquid from equilibrium [2]. The system is perturbed with a horizontal temperature gradient periodic along the height of the slot, and a constant vertical concentration gradient is imposed. The characteristic velocity U_c is taken to be the average of the magnitude of the velocity field across the mid-height of the slot. Equating the diffusive and convective time scales τ_D and τ_c (i.e., setting $\mathrm{Pe} = 1$) determines a crossover temperature gradient below which the authors expect the system to have a barodiffusion gradient signifying an effective equilibrium and above which they expect destruction of the barodiffusion gradient. The predictions of the model depend strongly on the geometry of the sample as well as the distance from the critical point. For a given width, a taller sample will be more susceptible to convection. As one moves away from the critical point, there are two competing effects: the size of the barodiffusion gradient decreases, which increases the characteristic velocity of the flow thus decreasing τ_c, and the diffusion coefficient increases, decreasing τ_D. The diffusion effect dominates, and in general the region of safe temperature gradients grows as the system moves away from the critical point. As an example of likely experimental situations, for a 1.5 cm square cell of near-critical carbon disulfide and nitromethane held about 1 K from its critical temperature, the region of safe temperature gradients is about ± 1 mK/cm; in a cell five times shorter, the range is about ± 5 mK/cm; and finally, if in this shorter cell the temperature is increased to 8 K above T_c, the range increases to about ± 35 mK/cm [12].

Gravitational effects in near-critical pure and binary fluids have been actively studied. Pure fluids near a gas–liquid critical point [13] develop density gradients due to gravity as a result of the divergent isothermal compressibility of the system. Near a liquid–liquid critical point, however, the isothermal compressibility is well-behaved while the osmotic compressibility diverges [8], leading to different phenomena in the two systems. Gravitational effects coupled with hydrodynamics have been investigated in studies of phase separation [14]. One such recent study employs a geometry very similar to the one used in the experiment presented here: Platten and Chavepeyer have investigated phase separation in the presence of applied horizontal temperature gradients which are large enough to drive one side of the system below its critical temperature [15]. Yet the Platten and Chavepeyer system is convection dominated ($\mathrm{Pe} \gg 1$), while the experiment we present here attempts to investigate the regions where Pe is of order unity or below and diffusion becomes more important.

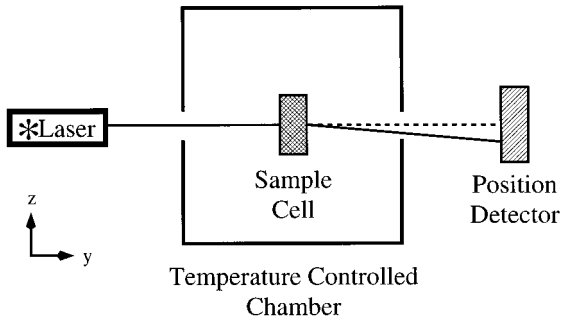

FIG. 1. Schematic of the experimental setup. Gravity points in the $-z$ direction.

Previous experimental investigations of diffusive gravity-induced concentration gradients in binary liquids have focused only on fast developing gradients where sedimentation dominates or on the measurement of equilibrium barodiffusion. A magnetic densimeter technique has been used in a rather tall (7.6 cm) sample with a long equilibration time to investigate sedimentation [16], and further studies of sedimentation and density inversion in large gravitational fields were performed using an ultracentrifuge and Schlieren imaging [17]. Giglio and Vendramini used a beam deflection technique [18], and Maisano, Migliardo, and Wanderlingh used an interferometric technique [19] to investigate the critical behavior of barodiffusion in samples short enough to equilibrate in reasonable times. In the present experiment, we reinvestigate the development of the equilibrium barodiffusion gradient and observe its evolution in the presence of thermal stirring provided by applied horizontal temperature gradients.

II. EXPERIMENT

A schematic diagram of our apparatus is shown in Fig. 1. Vertical concentration gradients in the sample are measured using a beam deflection technique similar to the one used in the earlier experiments of Giglio and Vendramini [18,20]. A He-Ne laser beam is directed through a critical-composition mixture of aniline and cyclohexane (0.403 vol % aniline [21]), which is held in the single-phase region about 206 mK above its critical temperature $T_c = 29.77°\mathrm{C}$ [22]. Any concentration gradient in the sample will lead to a gradient in the index of refraction of the mixture, causing the beam to de-

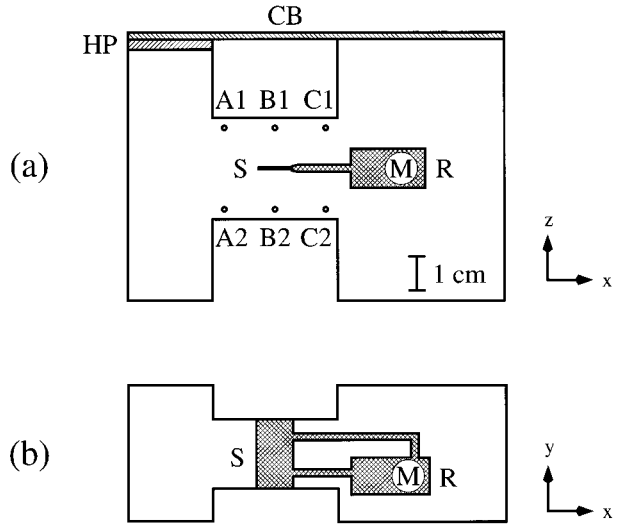

FIG. 2. (a) Side view of sample cell. (b) Top view of cell, showing a cross section through the center of the slot. *S*, sample slot; *M*, magnetic stirrer; *R*, reservoir; HP, heat pump; CB, copper bridge, *A*–*C*, holes for thermistor and thermocouple placement, present on each side of the aluminum block. The laser beam travels in the *y* direction. Windows and additional plugged holes used to drill channels and fill cell are not shown.

flect. The vertical deflection of the laser beam is measured with a single-axis position sensing photodiode [23] and is related to the vertical concentration gradient in the sample dc/dz by the expression [18]

$$\frac{dc}{dz}=\left(\frac{\partial n}{\partial c}\right)_{p,T}^{-1}\frac{\Delta z}{lL}, \tag{4}$$

where c is the mass fraction concentration of aniline, Δz is the beam deflection in the vertical direction (typically ranging from zero to 400–800 μm during a run), n is the index of refraction of the mixture, l is the depth of the sample along the direction of the beam path (20 mm), and L is the distance from the sample to the detector (94 cm). The value used for $(\partial n/\partial c)_{p,T}$ is 0.163 [24]. The position detector is 5 mm tall; 90% of the beam's power falls in a spot of height 1.6 mm on the detector.

A diagram of the side and overhead views of the sample cell is shown in Fig. 2. The sample of aniline and cyclohexane rests in a slot 10 mm wide $\times$ 1 mm high $\times$ 20 mm deep, which has been spark cut through an aluminum block. The slot is connected to a larger reservoir by two channels, and a teflon-covered magnetic stirrer in the reservoir can be translated by rotating a small magnet outside the sample cell. Glass windows are mounted to the front and back of the slot using indium gaskets. The laser beam, of diameter about 1.5 mm, is directed through the center of the slot; since the slot is only 1 mm high, it blocks part of the incoming beam. The laser power can be adjusted using a polarizer placed in the beam path.

The sample cell rests on a Delrin platform within a copper chamber whose temperature is actively controlled using a resistance thermometer and resistive strip heaters; a passive insulating box outside the copper box completes the thermostat. The temperature of the sample is monitored using a thermistor placed below the center of the slot [position $B2$ in Fig. 2(a)]. This arrangement keeps the temperature stable to within 0.8 mK rms during the growth of the barodiffusion gradients. The distance from the critical temperature, $T-T_c$, varies slightly from run to run due to a temperature drop of about 10–20 mK that occurs when the mechanical stirring is turned off during each run. This drop is complete within about two hours, though, while the run duration is typically twenty hours. The temperature of the sample for each run is taken to be the temperature after the temperature drops and stabilizes; for the presented data, $T-T_c$ ranges from 189 to 217 mK, with an average value of $T-T_c=206$ mK. The critical temperature drifted by less than 0.2 mK/day for the 150 days during which data were taken.

Both horizontal and vertical temperature gradients are measured with copper-constantan thermocouple pairs resting in small wells in the cell located in the positions shown in Fig. 2(a). A thermocouple pair placed across positions $A2$ and $C2$ measures the horizontal temperature gradients, while the vertical gradients are measured across positions $A1$-$A2$, $B1$-$B2$, and $C1$-$C2$. We are able to measure temperature gradients to better than ± 0.4 mK/cm. By comparing the thermocouple voltages at zero applied temperature gradient with the voltages of the shorted nanovoltmeters, we determine that at zero applied temperature gradient, any stray temperature gradients in the cell are less than 0.5 mK/cm.

A typical run consists of three stages: (i) The sample is mechanically stirred to ensure that it is homogeneous. (ii) The mechanical stirring ceases, allowing a concentration gradient to form due to barodiffusion. (iii) The mechanical stirring resumes, destroying the concentration gradient. During a run, a horizontal temperature gradient may be applied across the sample to perturb the system (''thermal stirring''). When applied, this temperature gradient is present during all three stages of the run. The mechanical stirring for stages (i) and (iii) is provided by the teflon-covered magnetic stirrer in the reservoir, which acts as a piston when translated by the external magnet.

The thermal stirring is generated by running a heat current horizontally across the sample. The current is provided by a thermoelectric heat pump mounted on one arm of the aluminum block which is thermally connected to the other arm with a copper strip [see Fig. 2(a)]. The size of the applied horizontal temperature gradients dT/dx are limited by two factors: phase separation of the sample and the existence of unwanted vertical temperature gradients.

First, if dT/dx is too large, one side of the sample can fall below the critical temperature and phase separate. This problem is most restrictive when the reservoir is held at the lower temperature ($dT/dx<0$), because the temperature gradient exists across the reservoir as well as the slot. The liquid in the reservoir will thus phase separate at lower values of dT/dx than will the liquid in the slot.

The second limitation, the problem of unwanted vertical temperature gradients, results from the asymmetry of the cell design—the heat pump produces a small vertical heat current across the slot as well as a horizontal one. These vertical temperature gradients are important because, as shown in Eq. (1), they can also contribute to the formation of concentration gradients (the Soret effect). (We avoid this concern for the applied horizontal gradients dT/dx because the cell is ten

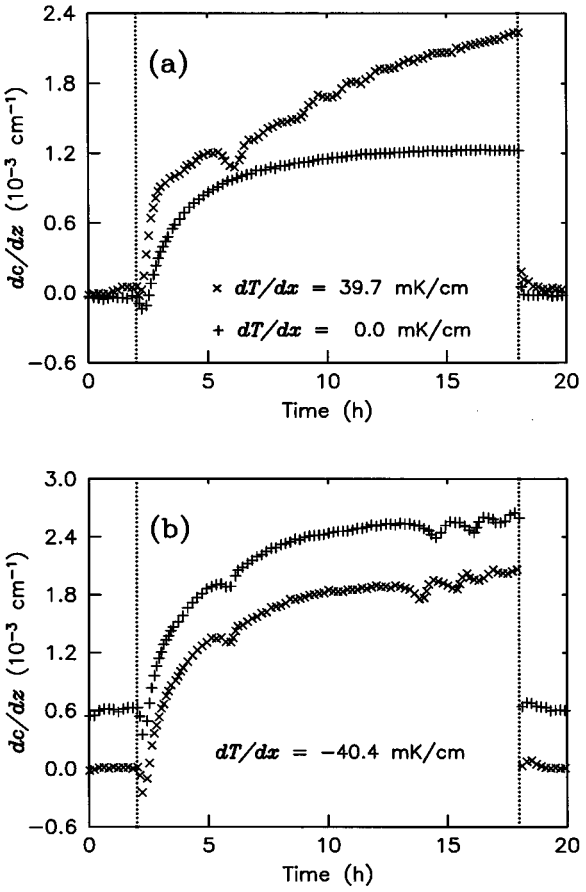

FIG. 3. (a) Two typical runs, the lower curve at $dT/dx=0$ ($T-T_c=207$ mK), the upper at $dT/dx=39.7$ mK/cm ($T-T_c=211$ mK). (b) Two consecutive runs at $dT/dx=-40.4$ mK/cm ($T-T_c=206$ mK) illustrating reproducible fluctuations on a fine time scale; the top curve has been shifted up for clarity. In each figure the dotted lines indicate the stopping and resumption of mechanical stirring.

times wider than it is tall, and thus, as shown by Eq. (3), the time for formation of horizontal concentration gradients is 100 times longer than the expected vertical diffusion time.) We carefully characterized the vertical temperature gradients at the center and sides of the slot, and using the Soret coefficient from Ref. [20], we conclude that the possible contribution of Soret gradients is significantly smaller than the observed concentration gradients. This effect will be discussed more completely with the presentation of the results. Consideration of the limitations of the thermal stirring led us to take data in the range $-40\leqslant dT/dx\leqslant 85$ mK/cm.

For the particular cell geometry, binary liquid, and value of $T-T_c$ used in this experiment, the characteristic velocity at crossover (when $\tau_D=\tau_c$) is $U_c\approx 0.1\mu$m/s. The previous work discussed above predicts that a horizontal temperature gradient of 34 mK/cm will provide such a flow [2].

III. RESULTS

The results of two typical runs, one with and one without an applied temperature gradient, are shown in Fig. 3(a). During time $t=$ 0–2 h, the system is mechanically stirred to ensure that the system is well mixed and that there is no vertical concentration gradient. At $t=2$ h, the mechanical stirring ceases, and a vertical concentration gradient begins to grow, reaching a steady value in the lower curve ($dT/dx=0$ mK/cm), but failing to do so during the duration of the run in the upper curve ($dT/dx=39.7$ mK/cm). At $t=18$ h, the mechanical stirring resumes, quickly destroying the concentration gradient. Data points are taken every 6 min, but have been thinned in the plots of Fig. 3 for clarity. The rms deviation of the beam in a well mixed sample, less than 10 μm, corresponds to a baseline rms deviation in the concentration gradients of less than 0.03×10^{-3} cm^{-1}.

The growth of these concentration gradients is not simple exponential growth, and many runs clearly exhibit much more complicated behavior. However, by assuming exponential decay for the runs which appear to reach a steady state, we can determine a characteristic e-fold growth time for the early behavior of these runs (using a value of 8.6×10^{-8} cm^2/s for the diffusion constant [25]). Earlier work (all performed with no applied temperature gradients) has had mixed agreement with the characteristic diffusion time [16,18,19]: that of Greer *et al.* observed time scales many times faster than those predicted by τ_D, that of Maisano *et al.* observed time scales two to three times faster than expected, and that of Giglio and Vendramini observed the expected time scales. The average value for the six points at $dT/dx=0$ (all of which reach a steady state) of $\tau_{\rm obs}=(3.5\pm1.3)$ h agrees with the expected value of $\tau_D=3.3$ h. Including the results of all the runs that came to a steady state the average characteristic growth time is (3.7 ± 1.1) h.

A summary of the results from all our runs is presented in Fig. 4. The concentration gradient dc/dz at $t=18$ h (the time at which the mechanical stirring resumes) is plotted against the applied horizontal temperature gradient dT/dx. The figure also includes the results in terms of the dimensionless concentration and thermal Rayleigh numbers, Ra_c and Ra_T [26]. In Fig. 4(a), the crosses indicate runs in which dc/dz reaches a steady value, and the open circles indicate runs in which dc/dz still appears to be changing when the mechanical stirring resumes. As mentioned earlier, the main source of error in these data is the possible contribution from Soret gradients. For $|dT/dx|<10$ mK/cm, the vertical temperature gradients (less than 0.6 mK/cm) lead to a possible contribution to dc/dz of less than 0.1×10^{-3} cm^{-1}. This error rises roughly linearly to 0.4×10^{-3} cm^{-1} at $|dT/dx|=40$ mK/cm, and at $|dT/dx|=85$ mK/cm, the error is about 1.0×10^{-3} cm^{-1}. Another consideration is the fact that the data were not all taken at exactly the same distance from T_c. By assuming a scaling with temperature that matches the equilibrium scaling, $dc/dz\sim|T-T_c|^{-1.2}$, we predict that the effect of the varying values of $T-T_c$ is smaller than 0.2×10^{-3} cm^{-1} for each data point.

Not presented with the data in Fig. 4 are the results of four runs during which unusually large concentration gradients formed, with values two to five times the average value at $dT/dx=0$. These runs were performed soon after the sample had phase separated (for example, after a measurement of the critical temperature). The large concentration gradients relax back to more consistent values over the three

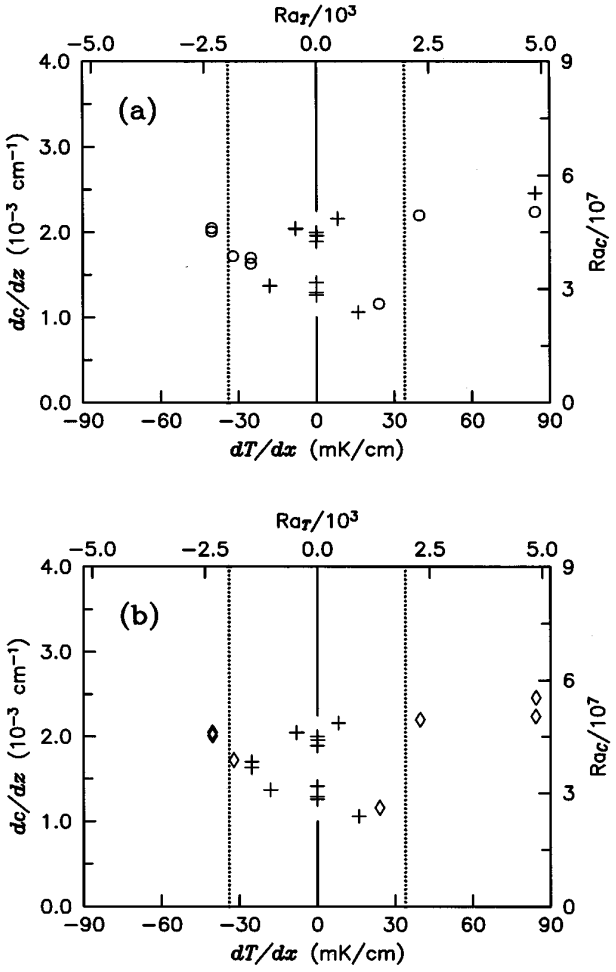

FIG. 4. Summary of barodiffusion gradient dc/dz at resumption of stirring versus applied horizontal temperature gradient dT/dx: (a) $+$, runs that come to a steady state concentration; $\bigcirc$, those which do not. (b) $+$, runs that do not have finer time scale features; $\diamond$, those which do exhibit such features. In each plot, the dotted lines indicate the crossover gradient predicted by Ref. [2] to give Pe$=1$. Uncertainties are discussed in the text. The average distance from T_c for the runs is $T-T_c=206$ mK.

days following phase separation. These residual effects persist for a surprisingly extended time, especially considering the fact that the sample is mechanically stirred while the temperature rises back above T_c.

The average value of dc/dz for the runs at zero applied temperature gradient is 1.6×10^{-3} cm^{-1}. This compares well with the previous experimental work of Giglio and Vendramini, which leads us to expect a value of $(1.4\pm0.2)\times10^{-3}$ cm^{-1} (estimating the error from the scatter in their presented data) at $T-T_c=206$ mK [18]. This value falls in the lower cluster of points at $dT/dx=0$ in Fig. 4. The value from the earlier work of Maisano *et al.*, for which we have not estimated an error, is smaller, 0.9×10^{-3} cm^{-1} [19].

In addition to the diffusive time scale, in more than one third of the runs we observe fluctuations in the concentration gradients which occur on finer time scales (finer even than the thermal relaxation time of about 2 h discussed above). Figure 4(b) designates those runs in which finer time scale features occur with an open diamond. These structures proved to be reproducible in the two cases which we were able to investigate: Fig. 3(b) shows the more striking case. The two runs in this figure, both at $dT/dx=-40.4$ mK/cm, were taken at staggered times on consecutive days and reveal significant fluctuations in the concentration gradient which occur at nearly identical times during the runs.

IV. DISCUSSION

While the behavior of the system does appear to change as the applied horizontal temperature gradient approaches the predicted crossover value (Pe$\rightarrow$1), the results presented in Fig. 4 do not confirm the expectations introduced earlier.

The dotted lines in Fig. 4 show the temperature gradient at which we expected to see convection begin to dominate diffusion (the crossover gradient). Outside of these lines on the figure, we expected to see dc/dz drop to values close to zero. Our limited choice of applied temperature gradients does not allow us to investigate fully the region beyond the predicted crossover: the three points at ±40 mK/cm are barely outside of the crossover region, and the two points at $+85$ mK/cm have a concentration gradient comparable to all the other gradients in the data set. It should be noted that in a previous data set, we did observe concentration gradients significantly smaller than the expected equilibrium value (but still nonzero) at large negative applied temperature gradients [27]. The predicted crossover temperature gradient does appear to have meaning, though, because the runs at larger values of dT/dx do not reach a steady concentration gradient within the duration of the run, and all the finer time scale fluctuations occur at larger temperature gradients as well. This suggests that convection could be playing a larger role in the system as the crossover gradient is approached, perturbing the system and slowing down the approach to a steady state.

Most strikingly, fluctuations dominate the data. Some introduction of noise could have been expected, since the presence of temperature gradients can drive the system from equilibrium, but even at zero applied temperature gradient, there are two clusters of data which vary from their average value by $\pm20\%$. While such fluctuations were not reported in the earlier work of Giglio and Vendramini and Maisano *et al.*, this behavior may not be totally without precedent—unpublished work and private communication with Giglio cited in Ref. [8] suggest that unwanted horizontal temperature gradients were suspected of having caused badly disturbed and unexpected behavior of concentration profiles in an experiment investigating Soret gradients.

We have eliminated Soret gradients, sample contamination, internal waves, and laser heating as causes of the unexpected behavior we have observed. First, one could imagine that Soret gradients could be enhancing the barodiffusion gradient, or that they could be growing up outside the laser beam and then somehow drifting into the beam path. As discussed earlier, however, we find that the vertical temperature gradients present in the sample are not large enough to explain the fluctuations in the barodiffusion gradient.

Next, there was a small amount of filamenty dustlike contamination restricted to a small volume around the bottom of one of the slot windows, but it is unlikely that this small contamination significantly affected the hydrodynamics

of the system. As for the chemical effects of the contamination, it has been shown that impurities only cause shifts in T_c: they do not seriously affect equilibrium and dynamic properties in the critical region in fluid mixtures, and further, they do not affect critical exponents [8]. Since the T_c drift of the sample was less than 0.2 mK/day for over 150 days, we conclude that the contamination did not affect the chemistry of the experiment.

We eliminate the possibility that internal waves are causing the observed behavior because the damping time of these oscillations is too short to be responsible for the fluctuations we see. Taking $\Delta\rho$ as the difference in density between the two liquids, ρ as the average density of the mixture, and $(dc/dz)_0$ as the vertical concentration gradient undisturbed by internal waves, the Brunt-Väisälä frequency, $N=[g(\Delta\rho/\rho)(dc/dz)_0]^{1/2}$, yields an oscillation period of about 10 s [28]. Assuming viscous damping of the internal waves, we estimate a damping time of about 0.1 s [29]. Thus these overdamped oscillations occur on a time scale much shorter than the time between each data point in a run, and would not be resolvable in the data. Further, calculating the energy of the lowest order ''sloshing'' mode waves that would result from equipartition, we estimate that the waves would only make a contribution to the observed barodiffusion gradient of $10^{-12}(dc/dz)_0$ [30].

Finally, we do not believe that laser heating contributes significantly to any features of the reported data. That a near-critical binary liquid is a delicate system is supported by the fact that increasing the laser power distinctly increases the noise in the beam deflection; we chose the laser intensity by reducing the intensity until we observed smooth data. The power of the beam incident on the sample cell is about 90μW, and the transmitted intensity is about 10μW. We can account for most of this attenuation (a reduction to about 30μW) by considering the aperturing of the beam by the slot, reflection from the windows, and the critical turbidity of the sample. There appears to be no correlation between laser intensity and the appearance of short time scale features in the data (which includes intensities that vary by about a factor of two), and further, it seems unlikely that laser heating would cause the reproducible behavior shown in Fig. 3(b). Concerning the fluctuations between runs, we have seen similarly large fluctuations at $dT/dx=0$ in three runs performed at more than twice the laser power of the data in Fig. 4, so we conclude that these fluctuations are independent of the laser intensity.

To investigate one aspect of the significance of the fluctuations observed at zero applied temperature gradient, we can approximate the effect that such fluctuations would have on a gravity-thinned wetting layer formed in a system at bulk two-phase coexistence. If the wetting attraction is due to dispersive forces, the wetting layer thickness l scales with the spectator phase height L as $l\sim L^{-1/3}$ for nonretarded dispersion and as $l\sim L^{-1/4}$ for retarded dispersion [31]. For screened electrostatic forces, $l\sim[-(1/2\kappa)\ln L+\text{const}]$, where κ^{-1} is the Debye screening length [32]. Both the spectator phase height L and the barodiffusion gradient dc/dz are proportional to the chemical potential, so that a change in dc/dz has the same effect as a change in L. Given these relations (and assuming a wetting layer thickness of about 100 nm and a screening length of about 10 nm for the case of screened electrostatic interactions), we estimate that a $\pm 20\%$ variation in the barodiffusion gradient will lead to a ∓ 1–5 % variation in the wetting layer thickness l.

While the effect on a wetting layer is small, it is important to note that it results from a fluctuation which occurs at zero applied temperature gradient in a system whose geometry is designed to restrict the effect of temperature gradients (recall that the predicted crossover gradient for this experiment is 34 mK/cm, while for other typical wetting experiments it can be near 1 mK/cm). Further, since many gravity thinned wetting experiments are performed at the liquid–vapor interface [4–6], in addition to bulk convection (which is no longer restricted at the top boundary by a no-slip boundary condition as it is in this experiment), the systems are also susceptible to surface (Marangoni) convection, making them even more sensitive to stray temperature gradients.

Beyond their relevance to wetting, though, the results suggest that even very small temperature gradients, corresponding to $\mathrm{Ra}_T<26$ (less than 0.5 mK/cm in this experiment), could provide a strong enough perturbation to drive a system from equilibrium or prevent it from attaining equilibrium within many diffusion times.

V. CONCLUSION

In studying barodiffusion in a binary liquid, we have observed behavior representative of the expected diffusion time at small applied temperature gradients; at larger temperature gradients, the characteristic time appears to become larger. The most striking features of the results are the fluctuations in the concentration gradients which occur in the steady state values at small temperature gradients, and which occur on finer time scales at larger temperature gradients. The fact that the barodiffusion gradient falls in a wide range of $\pm 20\%$ around its average value at zero applied temperature gradient (where we expect equilibrium behavior) suggests that very small temperature gradients may cause significant fluctuations in a binary liquid system.

One natural extension of this work would be to perform similar experiments in cells of varying geometry. Other work could also investigate perturbed barodiffusion at varying distances from the critical point as well as in different binary liquids. More detailed information about the concentration gradients and possibly the flow in the slot could be obtained by using an optical technique which provides more detailed spatial information.

Finally, the behavior we have observed is consistent neither with thermal noise, internal waves, nor the previous extension of Hart's theory. While the data do suggest that convection begins significantly to influence the system as the predicted crossover gradient is approached, the previous theory cannot predict the observed fluctuations. In both Hart's analysis and the extension made by Van Vechten and Franck, the vertical concentration gradient is an imposed constraint on the system; a more suitable analysis may include the vertical concentration gradient as a time-dependent variable. Also, while much work has been done on chemical waves in systems with thresholds for convection [33], our results suggest that studies of systems without such thresholds may reveal rich behavior as well.

ACKNOWLEDGMENTS

The authors wish to thank J. Breen for machining our sample cell and B. Carcich, R. Thorne, and D. Holcomb for lending us equipment. We are grateful to N. S. Desai, S. E. Peach, B. S. Schirato, R. D. Polak, and R. V. Durand for helpful discussions. T.C.V. wishes to acknowledge financial support from the Department of Education. Financial support was provided by the National Science Foundation through Grant No. DMR-9320910 and through MRL Central Facilities at the Materials Science Center at Cornell University (Grant No. DMR-9121654).

[1] X.-l. Wu, D. Ripple, and C. Franck, Phys. Rev. A **36**, 3975 (1987).

[2] T. C. Van Vechten and C. Franck, Phys. Rev. E **48**, 3635 (1993).

[3] R. F. Kayser, M. R. Moldover, and J. W. Schmidt, J. Chem. Soc. Faraday Trans. 2 **82**, 1701 (1986).

[4] D. Bonn, H. Kellay, and G. H. Wegdam, Phys. Rev. Lett. **69**, 1975 (1992); H. Kellay, D. Bonn, and J. Meunier, *ibid.* **71**, 2607 (1993).

[5] D. Bonn, H. Kellay, and G. H. Wegdam, J. Chem. Phys. **99**, 7115 (1993); D. Bonn, H. Kellay, and J. Meunier, Phys. Rev. Lett **73**, 3560 (1994).

[6] B. M. Law, Phys. Rev. Lett. **69**, 1781 (1992); **72**, 1698 (1994); Phys. Rev. E **48**, 2760 (1993); **50**, 2827 (1994); Ber. Bunsenges. Phys. Chem. **98**, 472 (1994); H. K. Pak and B. M. Law, Europhys. Lett. **31**, 19 (1995).

[7] L. D. Landau and E. M. Lifshitz, *Fluid Mechanics*, 2nd ed. (Pergamon, Oxford, 1987), Sec. 59.

[8] A. Kumar, H. R. Krishnamurthy, and E. S. R. Gopal, Phys. Rep. **98** (2), Sec. 7.3 (1983).

[9] D. J. Tritton, *Physical Fluid Mechanics*, 2nd ed. (Clarendon, Oxford, 1988), Chap. 4.

[10] D. A. Porter and K. E. Easterling, *Phase Transformations in Metals and Alloys* (VNR International, Berkshire, England, 1981), p. 72.

[11] J. E. Hart, J. Fluid Mech. **49**, 279 (1971).

[12] T. C. Van Vechten, Ph.D. thesis, Cornell University (University Microfilms, Ann Arbor, 1996).

[13] M. R. Moldover, J. V. Sengers, R. W. Gammon, and R. J. Hocken, Rev. Mod. Phys. **51**, 79 (1979).

[14] See, for example, F. Cau and S. Lacelle, Phys. Rev. E **47**, 1429 (1993) and references therein.

[15] J. K. Platten and G. Chavepeyer, Phys. Lett. A **174**, 325 (1993).

[16] S. Greer, T. E. Block, and C. M. Knobler, Phys. Rev. Lett. **34**, 250 (1975).

[17] T. E. Block, E. Dickinson, C. M. Knobler, V. N. Schumaker, and R. L. Scott, J. Chem. Phys. **66**, 3786 (1977).

[18] M. Giglio and A. Vendramini, Phys. Rev. Lett. **35**, 168 (1975).

[19] G. Maisano, P. Migliardo, and F. Wanderlingh, J. Phys. A **9**, 2149 (1976).

[20] M. Giglio and A. Vendramini, Phys. Rev. Lett. **34**, 561 (1975).

[21] D. Beaglehole, J. Chem. Phys. **73**, 3366 (1980). The cell was filled using a Pipetman P-1000 microliter pipette with an accuracy of 0.8%. The aniline was Fisher Scientific 99.9% assay; the cyclohexane EM Science OmniSolv 99.99% assay.

[22] The critical temperature is measured by lighting the slot from behind and observing the sample visually. T_c is taken to be the temperature at which the mixture is completely opaque. In most cases, the mixture is opaque over a range of about 12 mK; the critical temperature is taken to be the center of this range. Further, the mechanical stirring is on while T_c is being measured, so that in the phase-separated region, swirls of phase-separated droplets are easily visible. Although our thermometer has only an absolute calibration good to within 0.5°C, the measured T_c of 29.77 °C appears to agree well with the value of 29.55 °C reported in Ref. [21].

[23] The photodiode is a UDT Sensors model SL5-2. Following the manufacturer's recommendation, we run the diode with a reverse bias and normalize the signal with respect to the intensity, the position being given by the difference in anode currents divided by the sum of the anode currents.

[24] J. Timmermanns, *Physico-Chemical Constants of Binary Systems* (Interscience, New York, 1959), Vol. 1.

[25] P. Berge, P. Calmettes, B. Volochine, and C. Laj, Phys. Lett. **30A**, 7 (1969).

[26] These numbers are defined as $\mathrm{Ra}_c=(g\beta w^3 h/D\nu)(dc/dz)$ and $\mathrm{Ra}_T=(g\alpha w^4/\kappa\nu)(dT/dx)$ as in Ref. [11], except that we have chosen the height of the cell to be the characteristic length for dc/dz. In these expressions, β is the coefficient of volumetric expansion, α is the coefficient of thermal expansion, κ is the thermal diffusivity, ν is the kinematic viscosity, and h and w are the height and width of the slot, respectively.

[27] See T. C. Van Vechten, Ref. [12]. In this earlier data set, the sample was contaminated with a fine silt, and the typical run duration was about 24 h. This contamination was avoided in the present sample.

[28] See D. J. Tritton, Ref. [9], Sec. 15.4 for a discussion of internal waves.

[29] We estimate the damping time to be $h^2/(8\nu)$ by calculating the characteristic decay time of the angular velocity of a liquid in a cylindrical Couette cell of inner radius 0.9 cm and outer radius 1.0 cm; the density of the inner cylinder is taken to match the density of the liquid. A discussion of Couette flow is also present in Ref. [9], Sec. 9.3.

[30] The energy of a volume of liquid displaced a distance Δz is $U=\frac{1}{2}MN^2(\Delta z)^2$, where M is the mass of the displaced fluid. The ''sloshing'' mode will excite the entire fluid, so we take the mass to be ρ_0 times the total volume of the slot V_{tot}. Setting $U=\frac{1}{2}k_BT$ from equipartition, we have $(\Delta z)^2=(k_BT/N^2)(1/\rho_0 V_{\mathrm{tot}})$. This oscillation will tilt the direction of the concentration gradient by an angle of $\Delta z/W$ (where W is the width of the slot). For small oscillations, the vertical component of the gradient will then be $dc/dz=[1-(\Delta z/W)^2](dc/dz)_0$.

[31] I. E. Dzyaloshinskii, E. M. Lifshitz, and L. P. Pitaevskii, Adv. Phys. **10**, 165 (1961).

[32] R. F. Kayser, J. Phys. (Paris) **49**, 1027 (1988).

[33] M. C. Cross and P. C. Hohenberg, Rev. Mod. Phys. **65**, 851 (1993).